Front. Phys., 2012, 7(3): 315–318
DOI 10.1007/s11467-011-0207-y

RESEARCH ARTICLE

A broadband perfect field rotator

Qian-nan Wu, Ya-dong Xu, Huan-yang Chen†

School of Physical Science and Technology, Soochow University, Suzhou 215006, China

E-mail: †*chy@suda.edu.cn*

Received July 18, 2011; accepted August 11, 2011

In this letter, we design a perfect field rotator that is by itself invisible and can rotate the electromagnetic (EM) wave front. The device here is designed for a dielectric background and is composed of merely an inner core with the same dielectric and an array of metal plates embedded in the air. Its broadband functionality is also numerically demonstrated.

Keywords transformation optics, field rotator

PACS numbers 42.25.Fx, 41.20.Jb, 42.25.Gy

Transformation optics [1, 2] offer versatile tools to design devices with novel functionalities [3–6], including invisibility cloaks [7–17], field rotators [18], field concentrators [19], impedance-matched hyperlens [20], etc. Among them, only a few have been implemented, such as cloaks [7, 10, 11], carpet cloaks [13–16], field rotators [21], omnidirectional retroreflectors [22], extreme-angle lenses [23] and invisible gateways [24]. Field rotators [18], which come from rotation mapping, are invisible and can make objects inside them appear like rotated ones. Experimentally, an imperfect version [21] has been realized with simply an array of metal plates embedded in the air. Later on, layered structure [25] was proposed to design a perfect one, and has been applied to rotate liquid surface waves [26]. However, such a spiral layered structure is not easy to implement for EM wave. In this letter, we suggest a much simpler design of perfect field rotator for a dielectric background, which is composed of two kinds of isotropic materials. Numerical simulations are used to confirm its rotation effects in a broadband spectrum.

We start from the field rotator, which is of nonmagnetic response ($\mu_z = 1$) for transverse magnetic (TM) polarized waves (whose magnetic fields are along z- direction), and has a permittivity tensor [18, 21]

$$\overleftrightarrow{\varepsilon} = \begin{vmatrix} \varepsilon_{xx} & \varepsilon_{xy} \\ \varepsilon_{xy} & \varepsilon_{yy} \end{vmatrix} \tag{1}$$

where $\varepsilon_{xx} = \varepsilon_u \cos^2(\theta + \tau/2) + \varepsilon_v \sin^2(\theta + \tau/2)$, $\varepsilon_{xy} = (\varepsilon_u - \varepsilon_v)\sin(\theta + \tau/2)\cos(\theta + \tau/2)$, $\varepsilon_{yy} = \varepsilon_u \sin^2(\theta + \tau/2) + \varepsilon_v \cos^2(\theta + \tau/2)$, and $\varepsilon_u = (2 + t^2 - t\sqrt{t^2+4})/2$, $\varepsilon_v = (2 + t^2 + t\sqrt{t^2+4})/2$, $\cos\tau = \frac{t}{\sqrt{t^2+4}}$, $\sin\tau = \frac{2}{\sqrt{t^2+4}}$ (t is a constant here). The field rotator is invisible and can make objects inside it appear to be rotated images.

To implement such a device, we would like to introduce the following anisotropic unit cells, i.e., metal plates embedded in the air. For example, we suppose that the plates have rectangular cross sections with lengths $l_x = 1$ mm and $l_y = 5$ mm along x and y directions respectively. The unit cells are of a square shape with lengths $a = 6.25$ mm (we choose such unit cells for they will be used later). From the numerical simulations, we could retrieve the effective permittivity tensor, $\mathrm{diag}\{\varepsilon_x, \varepsilon_y\} = \mathrm{diag}\{1.19, 3.21\}$, and the effective permeability $\mu_z = 0.81$ for TM waves [21, 27] at a frequency of 8 GHz (or a wavelength of 37.5 mm, about 6 times of the sizes of the unit cells). Figure 1(a) shows the magnetic field distribution for a "point" source (excited by setting the magnetic field at a circular boundary $H_z = 1$ A/m) in front of an array of the above unit cells. The field pattern is similar to that of the source in front of an effective slab with the retrieved parameters, as plotted in Fig. 1(b). Therefore, the effective parameters we

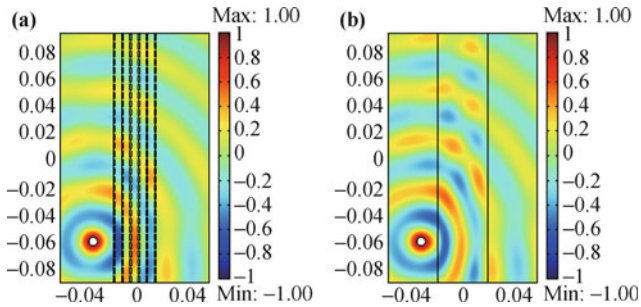

Fig. 1 The magnetic field distribution for a source in front of **(a)** an array of metal plates in the air, **(b)** an effective slab with retrieved parameters.

© Higher Education Press and Springer-Verlag Berlin Heidelberg 2012

extract here are reliable and could be useful in further designs.

Now, let us first use the above unit cells to design an imperfect field rotator like that in Ref. [21]. We will demonstrate that only an array of metal plates embedded in the air could perform the rotation effect (despite that the device is visible). The inner and outer radii of the field rotator are set to be 12.5 mm and 50 mm. The concentric shell is then divided into six shells, each with a thickness of 6.25 mm. Each shell can also be divided into unit cells each measuring 6.25 mm in the middle. The unit cells have "fanlike" shape (Readers can find a more detailed illustration in Fig. 1 of Ref. [21]). If a wavelength is large enough (e.g., 37.5 mm used here, which is much larger than 6.25 mm), the "fanlike" shape unit cells could be seen as the above square-shaped unit cells approximately. In the first step, the rectangular metal plates are placed in the center of each cell with the longer side aligned with the tangential direction (the θ- direction). Secondly, each plate is rotated anticlockwise around its center by an angle of $\tau/2$ (set to be 38° here). Figure 2 (a) shows the magnetic field distribution for such a device for an incident TM plane wave. In spite of some scattering, the device produces a wave front rotation effect (with about 40°). Figure 2(b) shows the scattering pattern for a device with $\varepsilon_u = 1.19$, $\varepsilon_v = 3.21$, $\tau = 76°$, yet with a magnetic response $\mu_z = 0.81$. The two similar field patterns demonstrate again the validity of the effect parameters. Now, let us keep the principal refractive indexes unchanged so that we could have a reduced device without magnetic response ($\mu_z = 1$ now). The principal permittivity values thus become $\varepsilon_u = 1.19 \times 0.81 = 0.964$ and $\varepsilon_v = 3.21 \times 0.81 = 2.6$. Figure 2(c) shows the scattering pattern for such a reduced device, deviating slightly from the pattern in Fig. 2(b). The reduced device here could be obtained by performing the rotation mapping to a dielectric concentric shell with a permittivity value $\bar{\varepsilon} = \sqrt{0.964 \times 2.6} = 1.58$. If the same mapping is performed to the vacuum, we can obtain a perfect field rotator with $\varepsilon'_u = 0.964/1.58 = 0.61$ and $\varepsilon'_v = 2.6/1.58 = 1.64$ (where $\varepsilon'_u \cdot \varepsilon'_v = 1$ and $t = 0.5$, which is why we set the above $\tau/2 = 38°$). Figure 2(d) shows the scattering pattern for the dielectric concentric shell, whose outer part is identical to that in Fig. 2(c) outside the device. From the resembling far field scattering patterns in each subfigure of Fig. 2, we can find that the devices in Figs. 2(a), (b), and (c) work as if they have an effect permittivity value [as that of Fig. 2(d)]. If we change the permittivity of the background and the inner core to be that value, the scattering would be reduced or even eliminated due to the impedance matching conditions.

For example, we plot the scattering field pattern in Fig. 3(a) by replacing the air background and inner core into a dielectric with a permittivity value of 1.58. The device now causes little scattering, which comes from the above reduction with the principal refractive indexes unchanged. Numerically, we find that a permittivity value of 1.4 offers a much better functionality (which could be regarded as a perfect one), as shown in Fig. 3(b). Such

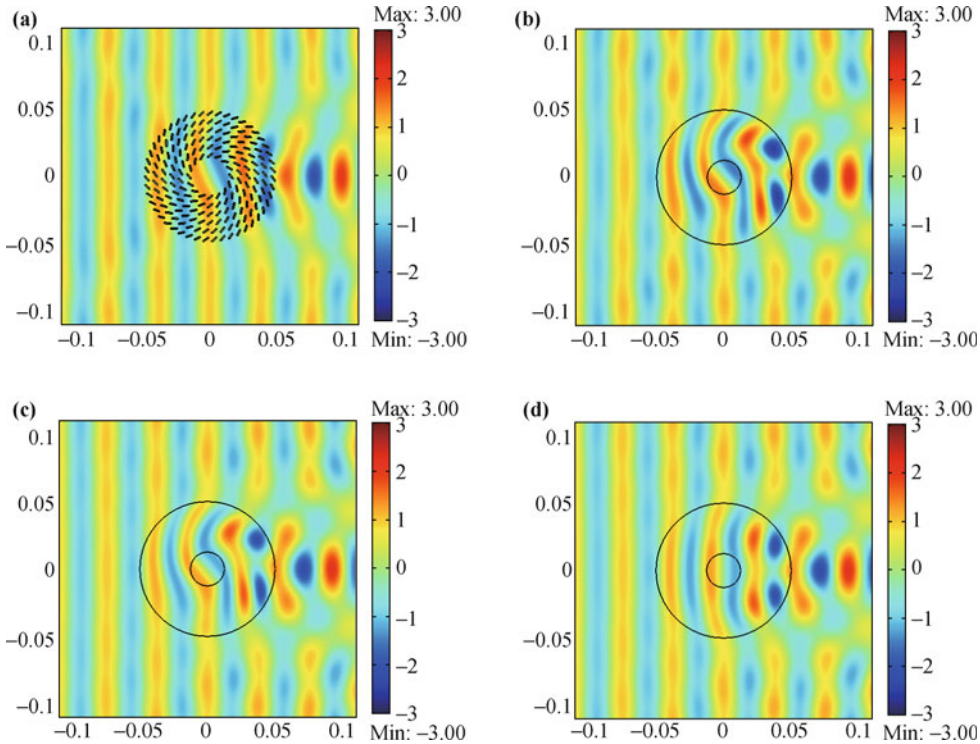

Fig. 2 The scattering pattern for **(a)** an imperfect field rotator composed of an array of metal plates in the air, **(b)** a device with $\varepsilon_u = 1.19$, $\varepsilon_v = 3.21$, and $\mu_z = 0.81$, **(c)** a device with $\varepsilon_u = 0.964$, $\varepsilon_v = 2.6$, and $\mu_z = 1$, **(d)** a dielectric concentric shell of $\bar{\varepsilon} = 1.58$.

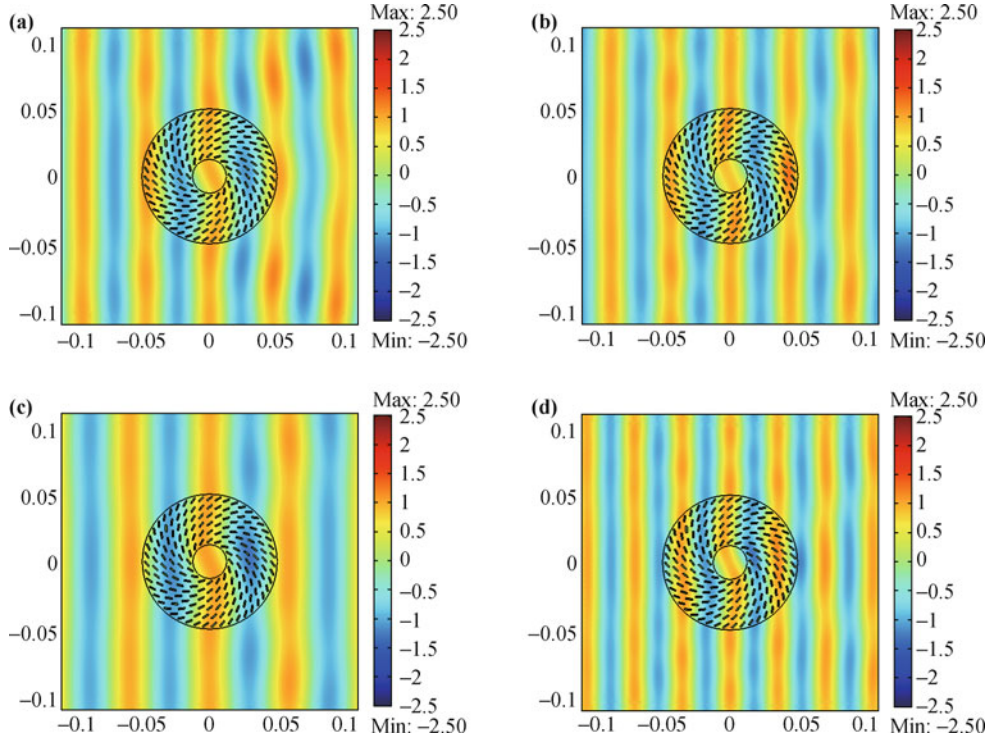

Fig. 3 The scattering pattern for the imperfect field rotator in Fig. 2(a) but with the air background and inner core replaced by a dielectric with a permittivity value of **(a)** $\bar{\varepsilon} = 1.58$ at 8 GHz, **(b)** $\bar{\varepsilon} = 1.4$ at 8 GHz, **(c)** $\bar{\varepsilon} = 1.4$ at 6 GHz, **(d)** $\bar{\varepsilon} = 1.4$ at 10 GHz.

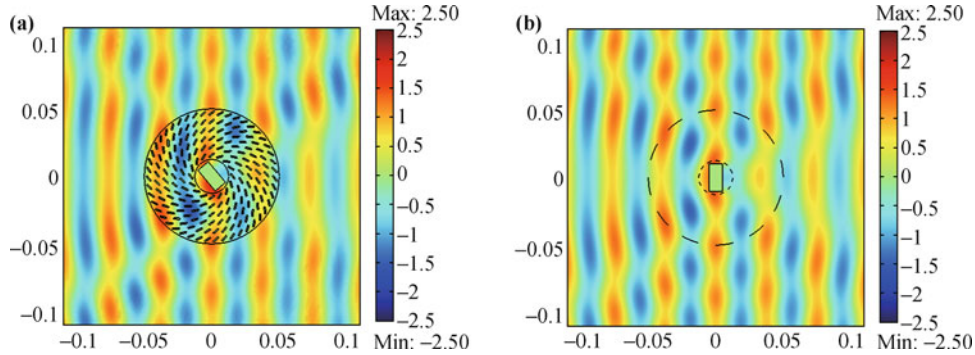

Fig. 4 The scattering pattern for **(a)** the designed perfect field rotator ($\bar{\varepsilon} = 1.4$) with a metal plate embedded inside the dielectric core, **(b)** a metal plate (but with a 40° rotation) embedded inside the dielectric ($\bar{\varepsilon} = 1.4$). The frequencies are set to be 8 GHz.

a device can also work in a broadband frequency range. For example, we plot in Figs. 3(c) and (d) the invisible behaviors for other frequencies (such as 6 GHz and 10 GHz respectively).

Finally, let us see what happens when we embed objects inside the dielectric inner core. Can the designed device perform good rotation effects [18]? Figure 4(a) shows the scattering pattern if a metal plate is embedded inside the inner core. The pattern is almost identical to that of the metal plate (yet rotated clockwise around its center by an angle of 40°) in the dielectric background, as shown in Fig. 4(b). Therefore, we illustrate here the good rotation effect using such a simple design.

In conclusion, we propose a design of broadband perfect field rotator. The device is designed for a dielectric background and is composed of merely a dielectric inner core and an array of metal plates in the air. It is so simple that it can not only work for microwave frequencies here but also could be easily extended to higher frequencies, such as terahertz or infrared frequencies [28, 29], except for some absorption from the metal plates.

Acknowledgements This work was supported by the National Natural Science Foundation of China (Grant No. 11004147), the Natural Science Foundation of Jiangsu Province (Grant No. BK2010211), and the Priority Academic Program Development (PAPD) of Jiangsu Higher Education Institutions.

References

1. U. Leonhardt, Science, 2006, 312: 1777
2. J. B. Pendry, D. Schurig, and D. R. Smith, Science, 2006, 312: 1780

3. V. M. Shalaev, Science, 2008, 322: 384
4. H. Y. Chen, C. T. Chan, and P. Sheng, Nat. Mater., 2010, 9: 387
5. X. Zhang and S. N. Zhu, Front. Phys., 2010, 5: 219
6. Y. Lai, J. Ng, H. Y. Chen, Z. Q. Zhang, and C. T. Chan, Front. Phys., 2010, 5: 308
7. D. Schurig, J. J. Mock, B. J. Justice, S. A. Cummer, J. B. Pendry, A. F. Starr, and D. R. Smith, Science, 2006, 314: 977
8. W. Cai and U. K. Chettiar, Nat. Photon., 2007, 1: 224
9. J. Li and J. B. Pendry, Phys. Rev. Lett., 2008, 101: 203901
10. S. Tretyakov, P. Alitalo, O. Luukkonen, and C. Simovski, Phys. Rev. Lett., 2009, 103: 103905
11. I. I. Smolyaninov, V. N. Smolyaninova, A. V. Kildishev, and V. M. Shalaev, Phys. Rev. Lett., 2009, 102: 213901
12. U. Leonhardt and T. Tyc, Science, 2009, 323: 110
13. R. Liu, C. Ji, J. J. Mock, J. Y. Chin, T. J. Cui, and D. R. Smith, Science, 2009, 323: 366
14. J. Valentine, J. Li, T. Zentgraf, G. Bartal, and X. Zhang, Nat. Mater., 2009, 8: 568
15. L. H. Gabrielli, J. Cardenas, C. B. Poitras, and M. Lipson, Nat. Photon., 2009, 3: 461
16. T. Ergin, N. Stenger, P. Brenner, J. B. Pendry, and M. Wegener, Science, 2010, 328: 337
17. Y. D. Xu, L. Gao, and H. Y. Chen, Front. Phys., 2011, 6: 61
18. H. Y. Chen and C. T. Chan, Appl. Phys. Lett., 2007, 90: 241105
19. M. Rahm, D. Schurig, D. A. Roberts, S. A. Cummer, D. R. Smith, and J. B. Pendry, Photon. Nanostruct. Fundam. Appl., 2008, 6: 87
20. A. V. Kildishev and E. E. Narimanov, Opt. Lett., 2007, 32: 3432
21. H. Y. Chen, B. Hou, S. Chen, X. Ao, W. Wen, and C. T. Chan, Phys. Rev. Lett., 2009, 102: 183903
22. Y. G. Ma, C. K. Ong, T. Tyc, and U. Leonhardt, Nat. Mater., 2009, 8: 639
23. N. Kundtz and D. R. Smith, Nat. Mater., 2010, 9: 129
24. C. Li, X. Meng, X. Liu, F. Li, G. Fang, H. Y. Chen, and C. T. Chan, Phys. Rev. Lett., 2010, 105: 233906
25. H. Y. Chen and C. T. Chan, Phys. Rev. B, 2008, 78: 054204
26. H. Y. Chen, J. Yang, J. Zi, and C. T. Chan, Europhys. Lett., 2009, 85: 24004
27. D. R. Smith, S. Schultz, P. Markoš, and C. M. Soukoulis, Phys. Rev. B, 2002, 65: 195104
28. P. Chaturvedi and N. X. Fang, Front. Phys., 2010, 5: 324
29. Y. Xie, H. Y. Chen, Y. Xu, L. Zhu, H. R. Ma, and J.W. Dong, Plasmonics, 2011, doi:10.1007/s11468-011-9226-3